Monte Carlo simulation of the Boltzmann equation for steady Fourier flow

J. M. Montanero, M. Alaoui, * A. Santos, and V. Garzó

Departamento de Física, Universidad de Extremadura, E-06071 Badajoz, Spain

(Received 20 July 1993; revised manuscript received 13 September 1993)

The planar Fourier flow for a dilute gas of hard spheres is studied by means of the direct-simulation Monte Carlo method to solve the Boltzmann equation. Two different types of boundary conditions are considered. In the conventional conditions, the gas can be seen as enclosed between two baths at equilibrium at wall temperatures. In the alternative conditions, both baths are out of equilibrium in states close to the one of the actual gas. It is shown that these alternative conditions are more appropriate to analyze bulk transport properties, as they reduce the boundary effects. The deviation of the heat flux from the Fourier law is small, even for large thermal gradients. In addition, the velocity distribution function is obtained and compared with the exact solution of the Bhatnagar-Gross-Krook model.

PACS number(s): 51.10.+y, 05.20.Dd, 05.60.+w

I. INTRODUCTION

The steady planar Fourier flow is one of the simplest macroscopic states for analyzing transport processes far from equilibrium. The physical situation corresponds to a system enclosed between two parallel infinite plates a distance L apart and kept at different temperatures T_- and T_+. Starting from an arbitrary initial state, the system reaches a steady state after a certain transient period. This steady state is characterized by a thermal gradient along the direction normal to the plates and a constant heat flux. At the level of the Navier-Stokes approximation, the heat flux and the thermal gradient are related through the phenomenological Fourier law

$$q_y^{\text{NS}} = -\kappa(T)\frac{\partial T}{\partial y} , \qquad (1.1)$$

where y denotes the coordinate along the direction normal to the plates and κ is the thermal conductivity coefficient. The Fourier law is expected to hold in the small gradient limit and in the bulk region, i.e., far away from the boundaries.

An interesting problem is to test the validity of the Fourier law beyond the linear regime in the bulk domain. This question has already been considered in computer simulations [1–3] as well as in kinetic theory descriptions [4–8]. Ciccotti and co-workers [1] performed molecular-dynamics simulations for a dense Lennard-Jones fluid in steady Fourier flow by using stochastic boundary conditions. No significant deviation from the Fourier law was observed up to gradients of the order of 1.8×10^9 K/cm for argon. Subsequently, Mareschal and co-workers [2] considered the same problem for a dilute hard-sphere gas, using molecular-dynamics and an approximate moment

method to solve the Boltzmann equation. They also concluded that the validity of the Fourier law extended outside the small-gradient domain. In these simulations the size of the system was small and, consequently, the influence of boundary effects on heat transport could be important. In addition, a homogeneous simulation method for producing heat flux in absence of a thermal gradient has also been proposed [3]. Nevertheless, its applicability might be restricted to situations very close to equilibrium [9]. On the other hand, these boundary effects are absent in an exact solution to the Boltzmann equation for Maxwell molecules [4]. In this solution, which applies to arbitrary thermal gradients in the bulk, the velocity moments of the distribution function are polynomials in the gradient. In particular, the pressure is constant and the heat flux is a linear function, i.e., it is exactly given by the Fourier law. Similar conclusions are obtained from a solution of the nonlinear Bhatnagar-Gross-Krook (BGK) kinetic model for general interactions [5]. Furthermore, the tractability of the BGK equation allows one to obtain explicitly the velocity distribution function [6]. Comparison of this solution with the one obtained numerically from the BGK equation for finite geometry [7] shows that the boundary effects give rise to a decrease of the heat flux with respect to the one given by the Fourier law. The reliability of the BGK model in the planar Fourier flow problem is supported [8] by comparison with molecular dynamics results [2].

A natural question is whether the exact validity of the Fourier law in an unbounded system of Maxwell molecules described by the Boltzmann equation extends to other interaction potentials. This question has an affirmative answer when the Boltzmann equation is replaced by the BGK approximation. Here, however, we want to consider the details of the Boltzmann collision term. Since the numerical solution of the Boltzmann equation by finite difference methods would be inadequate from a practical point of view, it is preferable to use the so-called direct-simulation Monte Carlo (DSMC) method [10]. This method is much more efficient from a computational point of view than the molecular-dynamics method

---

*Permanent address: Départment de Physique, Université Moulay Ismaïl, Meknès, Morocco.

for dilute gases.

In this paper, we use the DSMC method to solve the Boltzmann equation for a system of hard spheres in the planar Fourier flow. In the conventional boundary conditions, the gas is assumed to be enclosed between two baths *at equilibrium* at different temperatures. Under these conditions, a particle leaving the system is replaced by a particle coming from a bath at thermal equilibrium. Consequently, a mismatch between the velocity distribution of the reemitted particles and that of the particles located near the walls and moving along the same direction exists. In order to inhibit these boundary effects, we propose alternative stochastic boundary conditions. Now, the gas is assumed to be enclosed between two baths *out of equilibrium* described by the corresponding BGK solution to steady planar Fourier flow. A particle leaving the system is replaced by a particle coming from a (fictitious) gas in a nonequilibrium state similar to that of the actual system. Thus, the previous mismatch is expected to be much smaller.

The organization of this paper is as follows. A brief description of the planar Fourier flow and a summary of the results obtained from the BGK model are given in Sec. II. The DSMC method and some technical details are presented in Sec. III. The two types of boundary conditions mentioned above are described in detail in Sec. IV. In Sec. V we analyze the transient regime starting from three different initial conditions: two of global equilibrium at the wall temperatures, and one of local equilibrium. The final steady state is seen to be independent of the initial state, although the relaxation time towards the steady state is shorter in the case of a local equilibrium initial state. Once the steady state is reached, the quantities of interest are computed as time averages. Section VI is devoted to the profiles of temperature, pressure, and heat flux. It is observed that the temperature jump at the walls is smaller in the case of nonequilibrium boundary conditions than in the case of conventional boundary conditions. Further, the deviation from the Fourier law is less noticeable in the former case. In Sec. VII, the velocity distribution function in the bulk obtained from the simulation is compared with the one given by the BGK model. In general, the agreement is good although some discrepancies appear in the high velocity region. Finally, the conclusions are summarized in Sec. VIII.

II. PLANAR FOURIER FLOW

Let us consider a system enclosed between two parallel plates located at $y = 0$ and $y = L$. Both plates are maintained at constant temperatures T_- and T_+, respectively. The system is assumed not to be influenced by the action of gravitation, so that we can take $T_+ \geq T_-$ without loss of generality. Under these conditions, the system is driven out of equilibrium and a thermal gradient and a heat flux appear. If only gradients along the y direction exist and in the absence of convection along the x and z directions, the general hydrodynamic balance equations [11] become

$$\frac{d\rho}{dt} = -\rho \frac{\partial u_y}{\partial y} , \qquad (2.1)$$

$$\rho \frac{du_y}{dt} = -\frac{\partial P_{yy}}{\partial y} , \qquad (2.2)$$

$$\rho \frac{de}{dt} = -\frac{\partial q_y}{\partial y} - P_{yy} \frac{\partial u_y}{\partial y} . \qquad (2.3)$$

Here, ρ, $\rho\mathbf{u}$, and ρe are the densities of mass, momentum, and internal energy, respectively, $d/dt \equiv \partial/\partial t + \mathbf{u}\cdot\nabla$ is the substantial time derivative, P is the pressure tensor, and $\mathbf{q}$ is the heat flux vector. After a certain transient period, the system is expected to reach a steady state. In this regime, the balance equations imply that u_y, P_{yy}, and q_y are constant. Since the walls are fixed, the macroscopic velocity u_y vanishes in the steady state.

The balance equations (2.1)–(2.3) do not constitute a closed set. In situations near equilibrium, they become the Navier-Stokes hydrodynamic equations by assuming the Newton law for the pressure tensor and the Fourier law, Eq. (1.1), for the heat flux. In order to get microscopic expressions for the transport coefficients and analyze the domain of validity of the Navier-Stokes constitutive equations, it is appropriate to consider a dilute gas as a prototype system. In this case, a kinetic description is sufficient to characterize the state of the system by means of the velocity distribution function $f(\mathbf{r}, \mathbf{v}; t)$. This function obeys the Boltzmann equation, which reads [12–14]

$$\frac{\partial f}{\partial t} + \mathbf{v} \cdot \nabla f = J[f, f] , \qquad (2.4)$$

where

$$J[f, f] = \int d\mathbf{v}_1 \int d\widehat{\mathbf{k}}\, g\, I(g, \widehat{\mathbf{k}})[f' f_1' - f f_1] \qquad (2.5)$$

is the collision operator. In this equation, $I(g, \widehat{\mathbf{k}})$ is the differential cross section and $g \equiv |\mathbf{v} - \mathbf{v}_1|$ is the relative speed. At this kinetic level, the densities of conserved quantities and the fluxes can be expressed as velocity moments of f:

$$\rho = mn = m \int d\mathbf{v}\, f , \qquad (2.6)$$

$$\rho\mathbf{u} = m \int d\mathbf{v}\, \mathbf{v} f , \qquad (2.7)$$

$$\rho e = \tfrac{3}{2} n k_B T = \frac{m}{2} \int d\mathbf{v}\, (\mathbf{v} - \mathbf{u})^2 f , \qquad (2.8)$$

$$\mathsf{P} = m \int d\mathbf{v}\, (\mathbf{v} - \mathbf{u})(\mathbf{v} - \mathbf{u}) f , \qquad (2.9)$$

$$\mathbf{q} = \frac{m}{2} \int d\mathbf{v}\, (\mathbf{v} - \mathbf{u})^2 (\mathbf{v} - \mathbf{u}) f . \qquad (2.10)$$

Here, m is the mass of a particle, n is the number den-

sity, k_B is the Boltzmann constant, and T is the temperature. The ideal gas equation of state, $p = nk_BT$, is verified locally, $p \equiv \frac{1}{3}\text{tr}\mathsf{P}$ being the hydrostatic pressure. The Navier-Stokes transport coefficients can be obtained from the Chapman-Enskog method to solve the Boltzmann equation [12,13]. In particular, the thermal conductivity coefficient for hard spheres of diameter σ is [13]

$$\kappa = \frac{75}{64}\frac{(\pi mk_BT)^{1/2}k_B}{m\pi\sigma^2} \; . \qquad (2.11)$$

Thus, according to the Fourier law, $q_y^{\text{NS}} \propto \partial T^{3/2}/\partial y$ for a dilute gas of hard spheres. Consequently, the profile of $T^{3/2}$ is linear in the steady state described by the Fourier law.

The Chapman-Enskog method provides the so-called normal solution to the Boltzmann equation [12]. The normal solution describes the state of the gas in the hydrodynamic regime, namely, for times much longer than the mean free time and for distances from the walls much larger than the mean free path. In that regime, all the dependence of f on $\mathbf{r}$ and t is given through a functional dependence on the hydrodynamic fields n, $\mathbf{u}$, and T. On the other hand, in situations not accounted for by the normal solution, the Boltzmann equation must be solved subject to specific initial and boundary conditions. The boundary conditions corresponding to the particular geometry of the problem can be written as [12]

$$H(-v_y)|v_y|f(y = L, \mathbf{v}; t)$$

$$= H(-v_y)\int d\mathbf{v}' \, |v_y'|K_+(\mathbf{v}, \mathbf{v}')H(v_y')f(y = L, \mathbf{v}'; t) \; ,$$
$$(2.12)$$

$$H(v_y)|v_y|f(y = 0, \mathbf{v}; t)$$

$$= H(v_y)\int d\mathbf{v}' \, |v_y'|K_-(\mathbf{v}, \mathbf{v}')H(-v_y')f(y = 0, \mathbf{v}'; t) \; ,$$
$$(2.13)$$

where H is the Heaviside step function. When a particle with velocity $\mathbf{v}'$ hits the wall at $y = L$, the probability of being reemitted with velocity $\mathbf{v}$ in the range $d\mathbf{v}$ is given by $K_+(\mathbf{v}, \mathbf{v}')d\mathbf{v}$. The kernel $K_-(\mathbf{v}, \mathbf{v}')$ has a similar meaning at $y = 0$. The specific details of the boundary conditions are contained in the kernels. In the case of the Fourier problem, $K_\pm$ must be consistent with the temperature walls $T_\pm$.

As mentioned in the Introduction, an exact solution of the Boltzmann equation for Maxwell molecules in steady planar Fourier flow has been found [4]. As this solution belongs to the *normal* class, no explicit boundary conditions appear. All the space dependence of the velocity moments is given in terms of the local density and temperature and the local thermal gradient. The last can be defined in a reduced form as

$$\epsilon(y) \equiv \ell(y)\frac{\partial \ln T}{\partial y} \; , \qquad (2.14)$$

where $\ell(y)$ is a local mean free path. The dimensionless parameter ϵ measures the relative variation of temperature over a mean free path and characterizes the departure from equilibrium. Although the solution is valid for arbitrary values of ϵ, the pressure tensor coincides with that of equilibrium and the heat flux is linear in ϵ, so that the Fourier law is exactly verified.

More detailed information for this normal state can be obtained for arbitrary potentials if one uses the BGK equation as a kinetic model of the Boltzmann equation [5,6]. Again, the moments are polynomials in ϵ and, in particular, the heat flux is linear. Moreover, an explicit form for the velocity distribution function can be obtained [6]:

$$f(\mathbf{r}, \mathbf{v}) = n(m/2\pi k_BT)^{3/2}\frac{1}{\epsilon|\xi_y|}$$

$$\times \int_0^\infty dt \, H((1 - t)\text{sgn}\xi_y)t^{-5/2}$$

$$\times \exp\left(-\frac{1 - t}{\epsilon\xi_y} - \frac{\xi^2}{t}\right) \; , \qquad (2.15)$$

where

$$\boldsymbol{\xi} = (m/2k_BT)^{1/2}\mathbf{v} \qquad (2.16)$$

is the velocity relative to the local thermal velocity. Upon writing Eq. (2.15), the local mean free path has been identified as

$$\ell = \frac{2}{5}\frac{m\kappa}{pk_B}(2k_BT/m)^{1/2} \; . \qquad (2.17)$$

Equation (2.15) shows that the distribution function is a highly nonlinear function of the reduced thermal gradient. The series expansion of f in powers of ϵ is asymptotic but not convergent [6].

III. SIMULATION METHOD

As stated in the Introduction, our main goal is to assess the validity of the Fourier law for a dilute gas of particles interacting via a potential other than the Maxwell interaction. Since no analytic solution of the Boltzmann equation for this problem is known, we attack the problem by using a numerical approach. The most convenient method is the DSMC method [10]. In the simulation, the system (made of N particles) is split into cells of sizes much smaller than the mean free path. Time is advanced in discrete timesteps Δt, much smaller than the mean free time. The free motion and the collisions are uncoupled over the interval Δt: (i) All the molecules are displaced according to their velocity components. Those molecules crossing the boundaries are reentered with velocities sampled from a distribution given by the boundary conditions. (ii) Before proceeding to the next free displacement, a representative set of collisions, appropriate to Δt, is computed in each cell. The pre-collision velocities are replaced by random post-collision velocities. The choice of the representative set of collisions is governed by the potential model considered. Further de-

tails of the method can be found in Bird's monograph [10].

Given the geometry of the planar Fourier flow problem, the cells are taken as layers of width Δy and only the y coordinate of the particles needs to be stored. To check the validity of the Fourier law beyond the Maxwell interaction, specific interaction models must be considered. Here, we will restrict ourselves to hard spheres. The standard definition of mean free path in that case is

$$\lambda = \frac{1}{\sqrt{2}n\pi\sigma^2} \ . \tag{3.1}$$

Notice that $\ell = \frac{15}{16}\sqrt{\pi}\lambda$, where the BGK mean free path ℓ is given from Eqs. (2.11) and (2.17). We take the mean free path $\overline{\lambda}$, corresponding to the average density

$$\overline{n} = \frac{1}{L}\int_0^L dy\, n(y), \tag{3.2}$$

as length unit. Thus, the value of $L/\overline{\lambda}$ can be interpreted as an inverse Knudsen number. Other units are: $m = 1$ (mass unit), $(2k_BT_+/m)^{1/2} = 1$ (speed unit), $T_+ = 1$ (temperature unit), and $\overline{n} = 1$ (density level). Henceforth, all the quantities will be expressed in these units. Each different physical situation is characterized by its values of L and T_-. In terms of the above units, the reduced thermal gradient, Eq. (2.14), reads

$$\epsilon = \frac{5}{16}\sqrt{\pi}\frac{1}{p\sqrt{T}}\frac{\partial T^{3/2}}{\partial y} \ . \tag{3.3}$$

From the simulation data, the following quantities are computed at every time. The number of particles in layer α is

$$N_\alpha = \sum_{i=1}^N \Theta_\alpha(y_i) \ , \tag{3.4}$$

where y_i is the y-coordinate of particle i and $\Theta_\alpha(y)$ is the characteristic function of layer α, i.e., $\Theta_\alpha(y) = 1$ if y belongs to layer α and is zero otherwise. Similarly, the mean velocity, the temperature, the pressure, and the heat flux of layer α are evaluated, respectively, as

$$u_{y,\alpha} = \frac{1}{N_\alpha}\sum_{i=1}^N \Theta_\alpha(y_i)v_{i,y} \ , \tag{3.5}$$

$$N_\alpha k_B T_\alpha = \left(\frac{N}{L}\Delta y\right)p_\alpha = \frac{1}{3}m\sum_{i=1}^N \Theta_\alpha(y_i)v_i^2 \ , \tag{3.6}$$

$$P_{yy,\alpha} = m\left(\frac{N}{L}\Delta y\right)^{-1}\sum_{i=1}^N \Theta_\alpha(y_i)v_{i,y}^2 \ , \tag{3.7}$$

$$q_{y,\alpha} = \frac{1}{2}m\left(\frac{N}{L}\Delta y\right)^{-1}\sum_{i=1}^N \Theta_\alpha(y_i)v_i^2 v_{i,y} \ , \tag{3.8}$$

where $\mathbf{v}_i$ is the velocity of particle i. We have used $\mathbf{v}_i$

rather than the peculiar velocity $\mathbf{v}_i - \mathbf{u}$ in Eqs. (3.6)–(3.8) because in the steady state $\mathbf{u} = 0$, except for statistical fluctuations. Moreover, $P_{xx} = P_{zz} = \frac{1}{2}(3p - P_{yy})$ because of the geometry of the problem. The following global quantities are also computed:

$$\overline{u}_y = \frac{1}{N}\sum_{i=1}^N v_{i,y} \ , \tag{3.9}$$

$$\overline{p} = \frac{1}{3}m\frac{1}{N}\sum_{i=1}^N v_i^2 \ , \tag{3.10}$$

$$\overline{P}_{yy} = m\frac{1}{N}\sum_{i=1}^N v_{i,y}^2 \ , \tag{3.11}$$

$$\overline{q}_y = \frac{1}{2}m\frac{1}{N}\sum_{i=1}^N v_i^2 v_{i,y} \ . \tag{3.12}$$

The two first quantities are proportional to the total momentum and energy per particle, respectively.

Obviously, the accuracy, but also the computer time of the simulation, increase as N increases and Δy and Δt decrease. In our simulations, we have taken $N/L = 500$, $\Delta y = 0.1$, and $\Delta t = 0.003\,96$. We have observed that the results are especially sensitive to a bad choice of Δt. Figure 1 shows the time evolution of $\overline{u}_y$ for the case $L = 40$, $T_- = 0.05$ and three choices of Δt. The data obtained with $\Delta t = 0.017\,76$ clearly differ from those obtained with $\Delta t = 0.0088$ and $\Delta t = 0.0044$ and exhibit an unphysical growth of the average velocity. However, the data obtained with the two smaller values of Δt agree well within the statistical fluctuations.

IV. BOUNDARY CONDITIONS

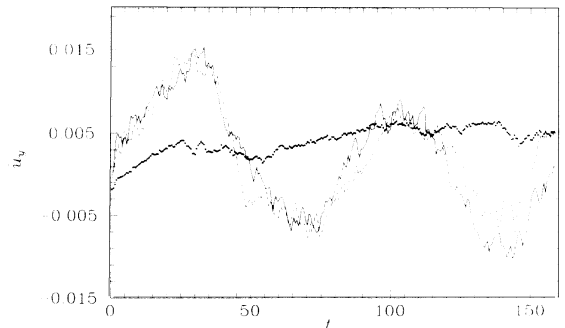In a bounded system, the boundary conditions play an essential role in determining the nonequilibrium state.

FIG. 1. Time evolution of the global average velocity $\overline{u}_y$ in the case $L = 40$, $T_- = 0.05$ for three choices of the time step: $\Delta t = 0.01776$ ($\cdots$), $\Delta t = 0.0088$ (- - -), and $\Delta t = 0.0044$ (—). In all cases, the initial condition is of global equilibrium at temperature $T_0 = T_+$ and the boundary conditions are of Type I.

In the context of the Boltzmann equation, these conditions are specified by the kernels $K_\pm$ [cf. Eqs. (2.12) and (2.13)]. In the case of complete accommodation with the walls, $K_\pm(\mathbf{v}, \mathbf{v}')$ does not depend on the incoming velocity $\mathbf{v}'$ and can be written as

$$K_\pm(\mathbf{v}, \mathbf{v}') \propto |v_y| \varphi_\pm(\mathbf{v}) H(\mp v_y) , \tag{4.1}$$

where the proportionality constant is obtained by normalization. The function $\varphi_+(\mathbf{v})$ can be interpreted as the probability distribution of a (fictitious) gas in contact with the system at $y = L$. The function $\varphi_-(\mathbf{v})$ allows a similar interpretation. Equation (4.1) means that when a particle hits a wall, it is replaced by a particle leaving from the fictitious gas. These functions account for the temperature of the walls, i.e.,

$$k_B T_\pm = \tfrac{1}{3} m \int d\mathbf{v}\, v^2 \varphi_\pm(\mathbf{v}) . \tag{4.2}$$

Usually, the functions $\varphi_\pm(\mathbf{v})$ are chosen as Gaussians:

$$\varphi_\pm(\mathbf{v}) = \left(\frac{m}{2\pi k_B T_\pm}\right)^{3/2} \exp(-\xi^2) , \tag{4.3}$$

where $\boldsymbol{\xi} = (m/2k_B T_\pm)^{1/2}\mathbf{v}$. These boundary conditions are used in molecular-dynamics simulations [1,2] and in kinetic theory analysis [7,8,14]. Under these conditions, the system is understood to be enclosed between two baths at equilibrium at temperatures T_+ and T_-, respectively. This type of condition is adequate if one is interested in studying realistic boundary effects [15]. However, they might not be the most convenient ones when the interest is focused on the transport properties in the bulk.

In order to inhibit the boundary effects, we propose here an alternative type of boundary condition. The idea is to imagine that the two fictitious gases are in nonequilibrium states resembling the nonequilibrium state of the actual gas near the contact surfaces. Since the distribution function of the actual gas is not known *a priori*, we assume that the fictitious gases are described by the distribution function given by the BGK approximation, Eq. (2.15). Thus, if the enclosed gas were also described by the BGK equation, no boundary effects would be present. More specifically, this second type of boundary condition is

$$\varphi_\pm(\mathbf{v}) = \left(\frac{m}{2\pi k_B T_\pm}\right)^{3/2} e^{-(\xi_x^2 + \xi_z^2)} \frac{1}{\epsilon_\pm |\xi_y|}$$

$$\times \int_0^\infty dt\, H((1-t)\mathrm{sgn}\xi_y) t^{-3/2}$$

$$\times \exp\left(-\frac{1-t}{\epsilon_\pm \xi_y} - \frac{\xi_y^2}{t}\right) . \tag{4.4}$$

Here, $\epsilon_\pm$ is the value of ϵ corresponding to a temperature $T_\pm$ and the thermal gradient predicted by the Fourier law. In our units,

$$\epsilon_\pm = \tfrac{15}{8}\sqrt{\pi}\, \frac{T_+^{1/2} - T_-^{1/2}}{L} T_\pm^{-1/2} . \tag{4.5}$$

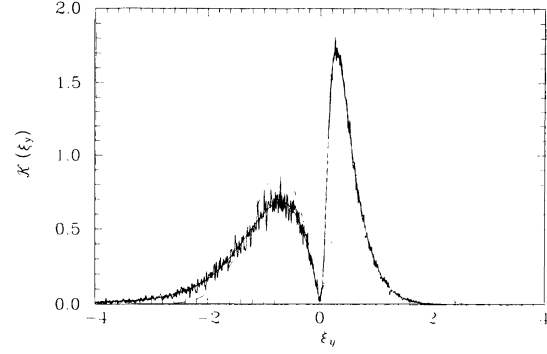For the sake of simplicity, we have assumed in Eq. (4.4) statistical independence among the three velocity com-

FIG. 2. Plot of the reduced kernels $\mathcal{K}_\pm(\xi_y)$ for boundary conditions of Type I (dashed line) and of Type II (solid line) in the case $L = 5$, $T_- = 0.05$. The fluctuating lines are simulation results for conditions of Type II.

ponents of the reemitted particle.

In the following, we will refer to the boundary condition (4.3) as a condition of Type I and to the boundary condition (4.4) as a condition of Type II. Figure 2 shows the reduced kernels

$$\mathcal{K}_\pm(\xi_y) = \left(\frac{m}{2k_B T_\pm}\right)^{-1/2} \int_{-\infty}^\infty dv_x \int_{-\infty}^\infty dv_z\, K_\pm(\mathbf{v}, \mathbf{v}') \tag{4.6}$$

for boundary conditions of Type I (dashed line) and of Type II (solid line) and the case $L = 5$, $T_- = 0.05$. While $\mathcal{K}_-(\xi_y) = \mathcal{K}_+(-\xi_y)$ for conditions of Type I, a strong asymmetry appears for conditions of Type II. In the latter case, particles reemitted from the hot wall ($\xi_y < 0$) have typically larger velocities (relative to the thermal velocity) than particles reemitted from the cold wall ($\xi_y > 0$). The noisy lines correspond to simulation results obtained using boundary conditions of Type II after about 74 000 collisions with the cold wall and 22 000 collisions with the hot wall. As expected, the collision frequency with the walls is larger in the case of the cold wall, where a smaller thermal velocity is compensated by a larger population.

Both conditions are schematically illustrated in Fig. 3. The dashed line represents the temperature profile predicted by the Fourier law without temperature jumps at the boundaries. The solid lines outside the system represent the temperature profiles of the fictitious gases, while
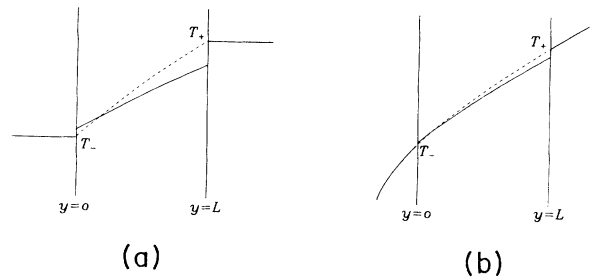
(a)   (b)

FIG. 3. Sketch of boundary conditions (a) of Type I and (b) of Type II.

the solid line inside the system is a qualitative representation of the expected profile. Although the boundary effects (represented by the temperature jumps at the walls) are unavoidable, they are expected to be less important in the case of boundary conditions of Type II.

V. TRANSIENT REGIME

By application of either of the above boundary conditions and after a sufficiently long time, the system is expected to reach a steady state independent of its initial preparation. In order to determine when the steady state has been reached, it is convenient to analyze the transient regime starting from different initial conditions. We have considered initial distribution functions of the form

$$f_0(y, \mathbf{v}) = n_0(y) \left(\frac{m}{2\pi k_B T_0(y)} \right)^{3/2} \exp\left(-\frac{mv^2}{2k_B T_0(y)} \right) ,$$

$$(5.1)$$

where the initial local number density $n_0(y)$ and temperature $T_0(y)$ have been chosen in three different ways: (a) $n_0(y) = \bar{n}$, $T_0(y) = T_+$, (b) $n_0(y) = \bar{n}$, $T_0(y) = T_-$, and (c) $n_0(y) \propto 1/T_0(y)$, $T_0(y) = T_-(1 + cy/L)^{2/3}$, $c \equiv (T_+/T_-)^{3/2} - 1$. The two first conditions correspond to a gas initially at equilibrium at the same temperature as that of one of the walls. In the third condition, the gas is initially prepared in a local equilibrium state described by the Navier-Stokes equations, namely, a constant pressure and a linear profile of $T^{3/2}$. As an illustration, Fig. 4 shows the time evolution of the global quantity $\bar{p}$ in the case $L = 10$, $T_- = 0.05$ for the three initial conditions and boundary conditions of Type I. The collisions with the walls are responsible for the absence of conservation of the total momentum and energy. Figure 4 shows that with conditions (a) and (b) the total energy monotonically decreases and increases, respectively, until reaching a common plateau; with condition (c), the total energy is initially quite close to the steady value.

From Fig. 4 and similar analysis of the evolution of $\bar{u}_y$ and $\bar{q}_y$, we conclude that the relaxation time to the

steady state lies between 100 and 200. In the sequel, we consider the initial condition (c) and assume that the steady state has been reached at $t = 200$. In order to reduce the influence of fluctuations, we follow the evolution of the system until $t = 400$ and take averages over 500 snapshots equally spaced between $t = 200$ and $t = 400$.

VI. HYDRODYNAMIC PROFILES: TRANSPORT PROPERTIES

To study the transport properties in the steady state, the following cases have been considered in the simulations: (a) $L = 10$, $T_- = 0.05$; (b) $L = 10$, $T_- = 0.01$; (c) $L = 5$, $T_- = 0.05$; and (d) $L = 20$, $T_- = 0.05$. In cases (a)–(c), boundary conditions of Types I and II have been used, while only conditions of Type II have been used in case (d). As an exact consequence of the conservation of mass, momentum, and energy, the corresponding fluxes must be spatially constant in the steady state, independent of the size and the boundary conditions of the system. We have checked that this fact is verified in our simulations. On the other hand, the conservation of momentum is compatible with $P_{xx} = P_{zz} \neq$ const. In the exact solutions of the Boltzmann equation for Maxwell molecules and the BGK equation in an unbounded system, one has $P_{xx} = P_{yy}$, which implies $p =$ const. The pressure profile obtained from simulation in the case $L = 10$, $T_- = 0.05$ and conditions of Types I and II is plotted in Fig. 5. The dashed lines are parabolic fits. It is apparent that a pressure gradient exists with both choices of boundary conditions. However, the shape of the pressure profile is clearly different in each choice. Since boundary effects are expected to be less important for conditions of Type II, we can conclude that a pressure gradient opposite to the temperature gradient is present in the bulk region of a hard-sphere gas. Surprisingly, the boundary effects seem to inhibit the inhomogeneity of pressure. It is interesting to note that the value of p averaged over space, i.e., $\bar{p}$, is very close to the value of $\overline{P}_{yy}$ when using both boundary conditions. This means that an equipartition theorem practically holds: $\langle v_x^2 \rangle \langle v_z^2 \rangle \simeq \langle v_y^2 \rangle$, where $\langle \rangle$ denotes a global average value
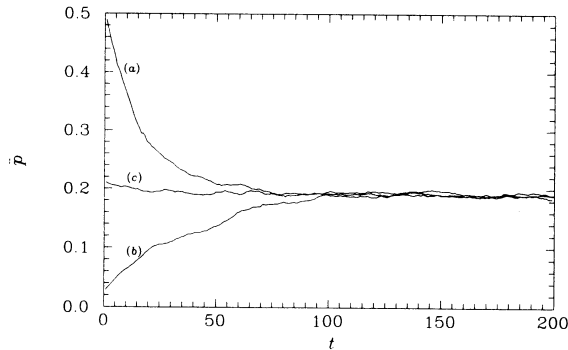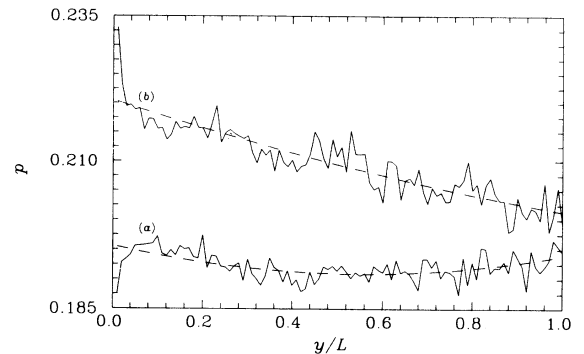

FIG. 4. Time evolution of the global average pressure $\bar{p}$ in the case $L = 10$, $T_- = 0.05$ for boundary conditions of Type I and three choices of the initial condition: (a) global equilibrium at temperature $T_0 = T_+$, (b) global equilibrium at temperature $T_0 = T_-$, and (c) local equilibrium described by the Navier-Stokes equations.

FIG. 5. Steady-state profile of the local hydrostatic pressure p in the case $L = 10$, $T_- = 0.05$ and boundary conditions (a) of Type I and (b) of Type II. The dashed lines are parabolic fits.
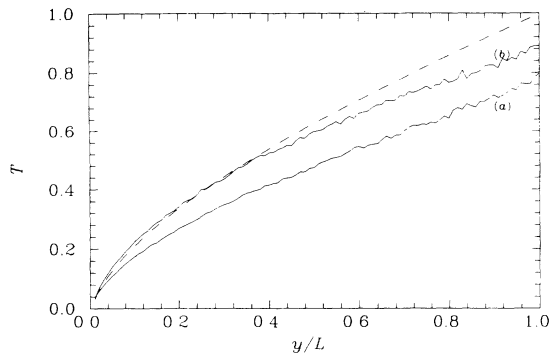
FIG. 6. Steady-state temperature profile in the case $L = 10$, $T_- = 0.01$ and boundary conditions (a) of Type I and (b) of Type II. The dashed line is the profile given by the Navier-Stokes equations with no-slip boundary conditions.
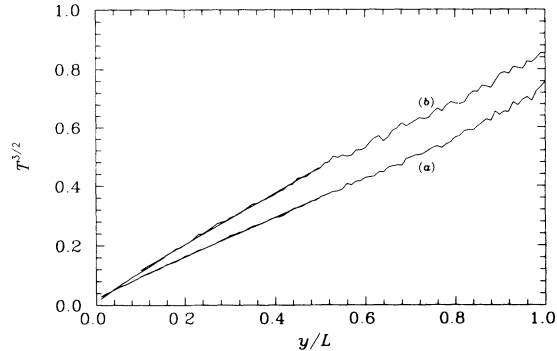

FIG. 7. Steady-state profile of $T^{3/2}$ in the case $L = 10$, $T_- = 0.05$ and boundary conditions (a) of Type I and (b) of Type II. The straight lines are linear fits in the region $0.1 < y/L < 0.5$.

per particle.

The most relevant hydrodynamic profile in this problem is that of the temperature. This profile is shown in Fig. 6 for the illustrative case $L = 10$, $T_- = 0.01$. The dashed line is the profile predicted by the Fourier law in the no-slip approximation. We observe that the temperature jumps at the walls are less important in the case of boundary conditions of Type II. This confirms the fact that these boundary conditions have a smaller influence on the transport properties than conditions of Type I. In our units, the Fourier law, Eq. (1.1), for a dilute gas of hard spheres can be written as

$$q_y^{\rm NS} = -\frac{25}{64}\sqrt{\pi}\frac{\partial T^{3/2}}{\partial y} . \qquad (6.1)$$

As a consequence, $T^{3/2}$ must be linear in the steady state. Figure 7 shows the profile of $T^{3/2}$ for the case $L = 10$, $T_- = 0.05$. In this representation, it is observed that both profiles are quasilinear. In order to compare the heat flux computed from simulation with the one given by the Fourier law, a bulk region where one can evaluate $\partial T^{3/2}/\partial y$ should be specified. This region must be separated from the walls by distances larger than the mean free path. For hard spheres, the mean free path near the hot wall is larger than the one near the cold wall. In all the cases considered, we have chosen the bulk region as $0.1L < y < 0.5L$. The straight lines in Fig. 7 correspond to linear regressions of $T^{3/2}$ in that interval.

The values of the most relevant quantities of the problem are shown in Table I for all the cases considered. The parameters ϵ_1 and ϵ_2 are the values of the reduced thermal gradient, Eq. (3.3), at $y = 0.1L$ and $y = 0.5L$, respectively. They give a measure of the departure from equilibrium of the region used to evaluate the Fourier heat flux, Eq. (6.1). In Fig. 8, each value of the ratio $q_y^{\rm NS}/\bar{q}_y$ is represented by a horizontal bar. The height is the statistical error and the width is the range $\epsilon_2 < \epsilon < \epsilon_1$. In all cases, the magnitude of the actual heat flux is smaller than that of the Navier-Stokes prediction, this effect being more noticeable in the case of boundary conditions of Type I. This indicates that boundary effects tend to decrease the heat flux across the system, in agreement with results derived from the BGK equation [7]. Anyway, in the case of boundary conditions of Type II, the deviation from the Fourier law is smaller than 10% even for values of ϵ as large as 0.8. It is important to point out that the deviation is about 33% in the case of boundary conditions of Type I, which are the ones used in previous simulations [1,2]. Since boundary effects are not completely eliminated by conditions of Type II, it is difficult to elucidate the contribution to the deviation from the Fourier law due to hydrodynamic nonlinear effects. However, comparison between cases (b) and (c) for conditions of Type II allows one to conjecture that the above contribution is smaller than 5% for values of the reduced thermal gradient ϵ around 0.8.

TABLE I. Simulation values of the most relevant quantities for all the cases studied. The statistical error is indicated in parentheses, in units of the last decimal place.

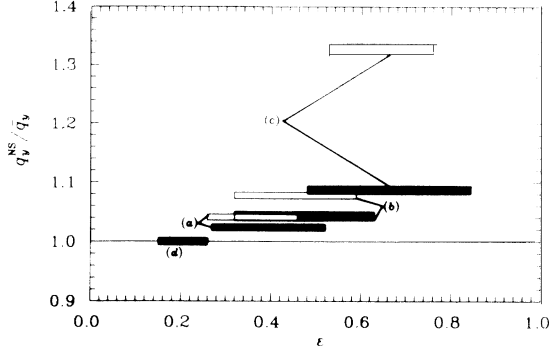| Boundary condition	L	T_-	$\overline{P}_{yy}$	$\bar{p}$	$\bar{q}_y$	ϵ_2	ϵ_1	$q_y^{\rm NS}$
I	10	0.05	0.1920(2)	0.1922(2)	0.0440(2)	0.26	0.46	0.0458
	10	0.01	0.1565(2)	0.1575(2)	0.0410(2)	0.32	0.59	0.0442
	5	0.05	0.1714(4)	0.1754(4)	0.0593(4)	0.53	0.76	0.0787
II	10	0.05	0.2123(3)	0.2098(6)	0.0585(3)	0.27	0.52	0.0599
	10	0.01	0.1864(2)	0.1843(6)	0.0584(4)	0.32	0.63	0.0609
	5	0.05	0.1962(4)	0.192(1)	0.0915(6)	0.48	0.84	0.0995
	20	0.05	0.2194(2)	0.2174(3)	0.0335(2)	0.15	0.26	0.0335

FIG. 8. Ratio between the heat flux given by the Fourier law and the actual heat flux for all the cases studied. Each value is represented by a horizontal bar of height equal to the statistical error and width equal to the range of the reduced thermal gradient ϵ corresponding to the region $0.1 < y/L < 0.5$. The empty and filled bars correspond to boundary conditions of Types I and II, respectively.
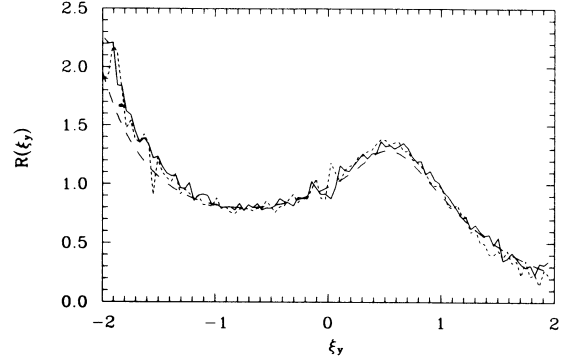

FIG. 9. Reduced distribution function $R(\xi_y)$ for a reduced thermal gradient $\epsilon = 0.334$. The two fluctuating lines correspond to the layer at $y = 0.30L$ in the case $L = 10$, $T_- = 0.05$ (solid line) and to the layer at $y = 0.42L$ in the case $L = 10$, $T_- = 0.01$ (dashed line), both with boundary conditions of Type II. The smooth dashed line corresponds to the exact solution of the BGK model.

VII. VELOCITY DISTRIBUTION FUNCTION

Besides the hydrodynamic quantities, the velocity distribution function can also be evaluated from the simulation. Given the geometry of the problem, it is convenient to define the reduced marginal distribution

$$R(\xi_y) = \frac{\int_{-\infty}^{\infty} dv_x \int_{-\infty}^{\infty} dv_z f(\mathbf{v})}{n\,(m/2\pi k_B T)^{1/2} \exp\left(-mv_y^2/2k_B T\right)} \,, \quad (7.1)$$

where the reduced velocity is defined in Eq. (2.16). It must be emphasized that in Eq. (7.1) the quantities n, T, and f are local. As said before, the state of the gas in the bulk is described by the normal solution to the Boltzmann equation. In this solution, all the space dependence of f is entirely contained in its functional dependence on the fields n and T. This means that, for a given value of ϵ, $R(\xi_y)$ must be independent of the details of the simulation. At the Navier-Stokes order, one has [13]

$$R^{NS}(\xi_y) = 1 - (\xi_y^2 - \tfrac{1}{2})\xi_y\epsilon \,. \quad (7.2)$$

The function R is plotted in Fig. 9 for $\epsilon = 0.334$. The two noisy lines correspond to the layer at $y/L = 0.30$ in the case $L = 10$, $T_- = 0.05$ and to the layer at $y/L = 0.42$ in the case $L = 10$, $T_- = 0.01$, both with boundary conditions of Type II. These two lines agree well within statistical errors. This confirms that in both cases the boundary effects are not important in the region we have taken as the bulk. On the other hand, both lines are clearly different from the Navier-Stokes prediction, Eq. (7.2), in spite of the fact that the heat flux is well described by the Fourier law. Figure 9 also shows the function R obtained from the BGK solution, Eq. (2.15). We observe that the BGK solution reproduces satisfactorily the general behavior of the distribution function. Nevertheless, some discrepancies are apparent in the region of high velocities and near the maximum. These differences tend to increase as ϵ increases, as shown in Fig. 10 for

$\epsilon = 0.68$. The simulation line corresponds to the layer at $y/L = 0.20$ in the case $L = 5$, $T_- = 0.05$.

VIII. DISCUSSION

In this paper we have addressed the planar Fourier flow problem for a dilute gas of hard spheres. The physical situation is that of a fluid enclosed between two parallel plates separated by a distance L and maintained at temperatures T_- and T_+. Since no analytic solution of the Boltzmann equation is known for this problem, we have solved it by means of the direct-simulation Monte Carlo method. Our main goal has been to analyze in the steady state the transport properties in the bulk region. In particular, we have been basically interested in checking the validity of the Fourier law in situations far from equilibrium. The Fourier law is exactly verified in the exact solutions of the Boltzmann equation for Maxwell molecules [4] and of the BGK model for general interac-
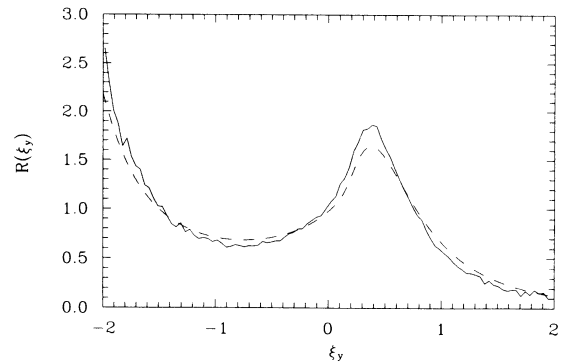

FIG. 10. Reduced distribution function $R(\xi_y)$ for a reduced thermal gradient $\epsilon = 0.68$. The solid line corresponds to the layer at $y = 0.20L$ in the case $L = 5$, $T_- = 0.05$. The dashed line corresponds to the exact solution of the BGK model.

tion potentials [5]. Both solutions refer to an unbounded system. In previous molecular-dynamics simulations of bounded systems (finite L) [1,2] the deviations from the Fourier law have been found to be small, even for large gradients. In those simulations, however, the influence of the boundary effects on the transport properties is not clearly elucidated.

In order to get a bulk domain, i.e., free from boundary effects, the natural idea is to take values of L much larger than the mean free path, i.e., small Knudsen numbers. There are, however, two drawbacks: (i) the relative temperature difference should be increased to keep a finite thermal gradient, and (ii) the number of particles and of layers in the simulation should increase, which is not convenient from a practical point of view. The boundary effects can also be diminished by choosing appropriate boundary conditions. In the conventional boundary conditions, used in previous works, each time a particle leaves the system, it is reemitted with a velocity sampled from a Gaussian probability distribution. An alternative idea is to consider a probability distribution for the reemitted particles similar to the actual velocity distribution function of the gas. More specifically, we have taken the analytic solution of the BGK model of the Boltzmann equation to define these new boundary conditions. In our simulations, we have considered Knudsen numbers of 0.05, 0.1, and 0.2 and temperature ratios of 0.01 and 0.05.

We have checked that the boundary effects are appreciably inhibited, but not eliminated, by the use of the boundary conditions. In contrast to what happens in the exact solutions of the Boltzmann equation for Maxwell molecules [4] and the BGK equation [5], the pressure is not constant in the bulk. The pressure gradient happens to be opposite to and of a much smaller magnitude than the thermal gradient. This is a nonlinear effect that is absent in the case of Maxwell molecules. On the other hand, when considering global average values, an equipartition theorem approximately holds: $\langle v_x^2 \rangle = \langle v_z^2 \rangle \simeq \langle v_y^2 \rangle$. Con-

cerning the temperature profile, it becomes quasilinear when plotting $T^{3/2}$, in agreement with the prediction of the Fourier law for hard spheres. By identifying the bulk region as the one lying between $0.1L$ and $0.5L$, we have computed the heat flux given by the Fourier law. Comparison with the heat flux measured directly in the simulations shows good agreement. We have estimated that for reduced thermal gradients close to 1, the deviations from the Fourier law not attributable to boundary effects is smaller than 5%. This conclusion does not imply that the state of the system is near equilibrium. In fact, the velocity distribution function obtained from simulation is highly distorted with respect to local equilibrium. Further, the distribution in the bulk region is practically independent of the details of the simulation and depends essentially on the local density, temperature, and thermal gradient. This is in accordance with the spirit of a normal solution. In addition, a comparison with the exact solution of the BGK model indicates good agreement, although the latter exhibits a smaller distortion.

Although in this paper we have restricted ourselves to dilute gases, we expect that the alternative boundary conditions introduced here are more useful than the conventional ones for studying transport properties in the bulk, even for dense fluids. Finally, the results obtained here encourage us to consider the planar Couette flow problem, where the corresponding BGK solution is also known [16].

ACKNOWLEDGMENTS

[1] G. Ciccotti and A. Tenenbaum, J. Stat. Phys. **23**, 767 (1980); A. Tenenbaum, G. Ciccotti, and R. Gallico, Phys. Rev. A **25**, 2778 (1982).

[2] M. Mareschal, E. Kestemont, F. Baras, E. Clementi, and G. Nicolis, Phys. Rev. A **35**, 3883 (1987); P.-J. Clause and M. Mareschal, Phys. Rev. A **38**, 4241 (1988).

[3] M. J. Gillan and M. Dixon, J. Phys. C **16**, 869 (1983); D. J. Evans, Phys. Lett. A **91**, 457 (1982).

[4] E. S. Asmolov, E. M. Makashev, and V. I. Nosik, Dok. Akad. Nauk SSR **249**, 577 (1979) [Sov. Phys. Dokl. **24**, 892 (1979)].

[5] A. Santos, J. J. Brey, and V. Garzó, Phys. Rev. A **34**, 5047 (1986).

[6] A. Santos, J. J. Brey, C. S. Kim, and J. W. Dufty, Phys. Rev. A **39**, 320 (1989).

[7] C. S. Kim, J. W. Dufty, A. Santos, and J. J. Brey, Phys. Rev. A **39**, 328 (1989).

[8] C. S. Kim and J. W. Dufty, Phys. Rev. A **40**, 6723 (1989).

[9] V. Garzó and A. Santos, Chem. Phys. Lett. **177**, 79

(1991).

[10] G. Bird, *Molecular Gas Dynamics* (Clarendon, Oxford, 1976); K. Nanbu, in *Rarefied Gas Dynamics*, edited by V. Boffi and C. Cercignani (Teubner, Stuttgart, 1986), pp. 369-383.

[11] S. R. de Groot and P. Mazur, *Non-Equilibrium Thermodynamics* (North-Holland, Amsterdam, 1962).

[12] J. R. Dorfman and H. van Beijeren, in *Statistical Mechanics, Part B*, edited by B. J. Berne (Plenum, New York, 1977), pp. 65-179.

[13] S. Chapman and T. G. Cowling, *The Mathematical Theory of Nonuniform Gases* (Cambridge University Press, Cambridge, 1970).

[14] C. Cercignani, *Mathematical Methods in Kinetic Theory* (Plenum, New York, 1990).

[15] D. C. Wadsworth, Phys. Fluids A **5**, 1831 (1993).

[16] J. J. Brey, A. Santos, and J. W. Dufty, Phys. Rev. A **36**, 2842 (1987); C. S. Kim, J. W. Dufty, A. Santos, and J. J. Brey, Phys. Rev. A **40**, 7165 (1989).